Synthesis and characterization of new fluorescent two-photon absorption chromophores†

Ping-Hsin Huang,[acd] Jiun-Yi Shen,[a] Shin-Chien Pu,[b] Yuh-Sheng Wen,[a] Jiann T. Lin,*[a] Pi-Tai Chou*[b] and Ming-Chang P. Yeh*[c]

Received 5th September 2005, Accepted 10th November 2005
First published as an Advance Article on the web 5th December 2005
DOI: 10.1039/b512524c

A series of dipolar and quadrupolar type two-photon absorption (TPA) compounds has been synthesized and TPA cross sections (σ) were measured by Ti:sapphire femtosecond laser excitation fluorescence (λ = 800 nm). Among them, the compound [2,5-bis-[5-(4-diphenylaminophenylethynyl)thiophen-2-yl]-[1,3,4]oxadiazole], **12**, has been structurally characterized by X-ray crystallography. The resulting data indicate that the structure of this compound possesses excellent coplanarity. The compounds have arylamines as the donor, and [1,3,4]oxadiazolyl, cyanovinyl or pyridazin-3,6-diyl moiety as the acceptor. Variation of arylamines and pendant alkyl groups was found to have a significant influence on σ values. By an appropriate combination of donor and acceptor, σ values of $>10^3$ GM (10^{-50} cm^{4}s photon·molecule^{-1}) can be achieved. One quadrupolar molecule (**13**) possessing an arylamine donor and a pyridazine acceptor has both a high σ value (1442 GM) and σ/MW (1.97 GM/g).

Introduction

With potentially large two-photon absorption (TPA) cross sections, organic conjugated compounds have been considered as a critical class of chromophores in nonlinear optics over past decades.[1,2] There is a growing interest in the development of new organic materials[3] having two-photon absorption cross sections for optical applications in a variety of new fields such as optical power limiting, two photon up-converted lasing, three-dimensional optical data storage, fluorescence imaging of biological samples, microfabrication and photodynamic therapies,[4–16] *etc*.

In recent years significant progress has been made on the development of organic conjugated molecules with large TPA cross sections.[15–31] Three classes of compound were found to be potential TPA chromophores; (1) dipolar type[17] with a donor–bridge–acceptor (D–π–A) motif; (2) quadrupolar type[18–27] with a D–π–D, A–π–A, D–π–A–π–D or A–π–D–π–A motif; (3) octupolar type[28–30] with a three-branched dipoles. Based on these studies, it was concluded that structural elements, which increase the effective conjugation length and polarizability of the molecules, should increase the TPA cross sections. Accordingly, coplanarity of the conjugation bridge is beneficial to increasing effective conjugation and polarizability. Furthermore, it is advantageous to have the two-photon peak at, or near, 800 nm, the wavelength used by most TPA microscopy, because most organic and biological materials have large optical transparency in this region. Greater penetration depth in tissue with reduced photodamage, while avoiding background fluorescence becomes viable for microscopic imaging. Therefore, in the ideal molecular design of TPA chromophores the two-photon absorption peak should not be shifted away from 800 nm while increasing the TPA cross section in order to avoid one-photon absorption.

A large number of reports on TPA molecules focus on variation of the conjugation bridge. In comparison, systematic variation of donors and acceptors has been much less explored,[15,17a,17e,30d] though it is well known that an appropriate combination of both factors will significantly affect the polarizability of the molecule. In this report, the synthesis and characterization of new two-photon chromophores using different donors and acceptors will be presented, among which the unusual influence of different arylamines on the TPA cross sections is of particular interest.

Results and discussion

Synthesis and characterization

Our initial aim of this research was to evaluate the possibility of tuning the TPA cross sections by variation of electron donors and acceptors. Three different arylamines were used as donors in both dipolar (**1–6**) and quadrupolar compounds (**7–13**). Different electron-deficient moieties, [1,3,4]oxadiazolyl, cyanovinyl, and pyridazin-3,6-diyl were used as electron acceptors. Syntheses of the new compounds in this study are illustrated in Schemes 1–3. The key reactions used for the construction of these conjugated molecules are palladium-catalyzed Sonogashira coupling,[32] Stille's cross-coupling[33] and a palladium catalyzed aromatic C–N coupling reaction,[34] *etc*. These compounds were isolated in 49–83% yields and are

[a]*Institute of Chemistry, Academia Sinica, Taipei, Taiwan 115, Republic of China. E-mail: jtlin@chem.sinica.edu.tw; Fax: +886-2-27831237; Tel: +886-2-27898522*
[b]*Department of Chemistry, The National Taiwan University, Taipei, Taiwan 106, Republic of China*
[c]*Department of Chemistry, National Taiwan Normal University, Taipei, Taiwan 116, Republic of China*
[d]*Kang-Ning Junior College of Medical Care and Management, Taipei, Taiwan 114, Republic of China*
† CCDC reference numbers 282997. For crystallographic data in CIF or other electronic format see DOI: 10.1039/b512524c

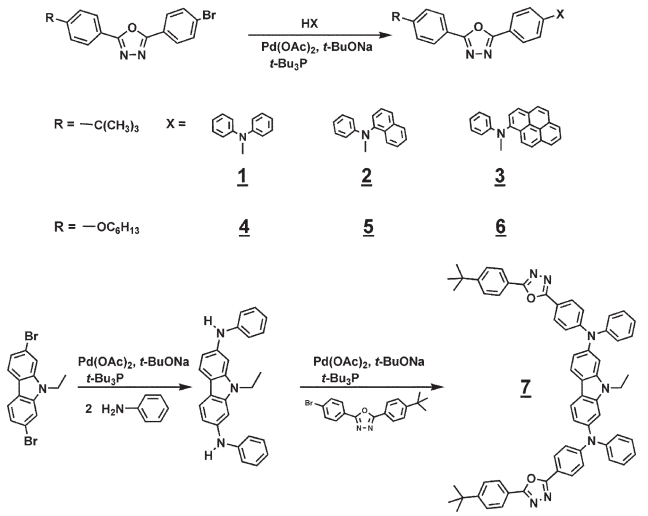

Scheme 1

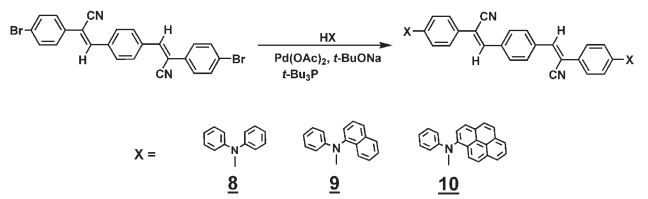

Scheme 2

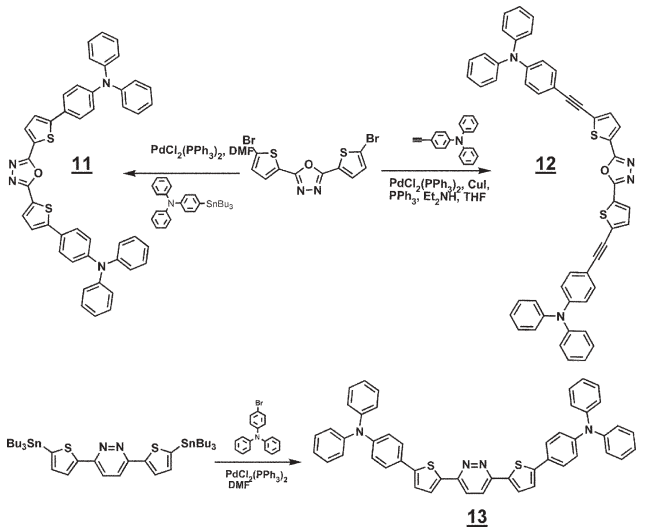

Scheme 3

soluble in common organic solvents. They were fully characterized by ^{1}H NMR, mass spectra and elemental analysis. X-ray structural data of compound **12** were also determined (*vide infra*).

Linear absorption and single-photon-excited fluorescence (SPEF)

The single-photon absorption and emission data of the compounds are presented in Table 1. Typical linear absorption and SPEF spectra of the compounds are displayed in Fig. 1 for

Table 1 One- and two-photon properties of **1–13** and references

Cpd	abs. $\lambda^{(1)}_{abs}$ [a] / nm	Φ [b]	abs. $\lambda^{(2)}_{abs}$ [c] / nm	TPEF $\lambda^{(2)}_{em}$ [d] /nm	TPA σ [e,f,g] / GM
1	354	0.55	800	451	98.36(0.22)
2	359	0.48	800	454	104.2(0.23)
3	380	0.47	800	461	135.0(0.24)
4	350	0.40	800	440	141.0(0.29)
5	358	0.35	800	446	143.3(0.27)
6	378	0.34	800	462	249.2(0.41)
7	386	0.17	800	524	575.6(0.62)
8	453	0.45	800	611	254.3(0.38)
9	457	0.26	800	620	540.8(0.71)
10	461	0.05	800	645	1180(1.29)
11	409	0.66	800	511	1390(1.93)
12	416	0.71	800	525	996.8(1.30)
13	433	0.60	800	536	1442(1.97)
C-480		0.87	800		168.2
R-6G		0.98	800		38.67

[a] $\lambda^{(1)}_{abs}$ of the one-photon absorption spectra in nm. [b] Fluorescence quantum yield. [c] $\lambda^{(2)}_{abs}$ of the two-photon absorption spectra in nm. [d] $\lambda^{(2)}_{em}$ of the two-photon emission spectra in nm. [e] TPA cross-section in 10^{-50} cm^4 s photon^{-1} (GM). [f] Numbers in the parenthesis are relative σ/MW. [g] Sample measured in CH_2Cl_2 at a concentration of 10^{-4} M, Coumarin 480 **(C-480)** and Rhodamine 6G **(R-6G)** measured in MeOH at a concentration of 10^{-4} M. **1–7** and **11–13** compare to Coumarin 480; **8–10** compare to Rhodamine 6G.

13 in CH_2Cl_2. All of the compounds have absorption cut-off below ~550 nm, indicating that there will be no linear absorption when laser source of 800 nm is used for TPA applications. The positions of the fluorescence peaks of these compounds are independent of the excitation wavelength in the absorption region and the quantum yields are also independent of the excitation wavelength from 360 nm to 450 nm.

The results indicate that the single-photon absorption maximum ($\lambda^{(1)}_{abs}$) of **1–3**, **4–6** and **8–10** increases in order of donor strength, pyrenylamino > naphthylamino > phenylamino.[35] Though compounds **7** and **1** possess a common conjugation segment for the charge transfer, the former has a larger $\lambda^{(1)}_{abs}$, possibly due to the stronger donating power of the carbazolyl moiety than that of the phenyl moiety. The electronic influence from the other peripheral amine and the

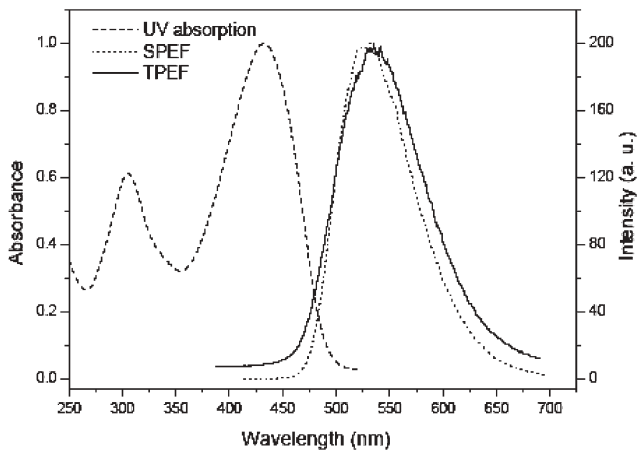

Fig. 1 The UV absorption and single-photon-excited fluorescence (SPEF) spectra (c = 5.0 × 10^{-6} M) and the two-photon-excited fluorescence (TPEF) (c = 1.0 × 10^{-4} M) of **13** in CH_2Cl_2.

longer conjugation length may also contribute to the increment of $\lambda^{(1)}_{abs}$ in **7**. Compound **11** has a much larger $\lambda^{(1)}_{abs}$ (409 nm) than **1** (354 nm) and **4** (350 nm) due to the interposition of a thiophene unit. It is well documented that insertion of thiophene in the conjugated segments results in better conjugation.[36] Similarly to our previous observation on benzo[1,2,5]thiadiazole-based molecules with peripheral amines,[37] the symmetrical nature of **11** will further enhance the charge transfer compared with **1** and **4**. The larger $\lambda^{(1)}_{abs}$ value in **12** (416 nm) than in **11** (409 nm) can be attributed to the elongation of the conjugation chain. The crystal structural determination on **12** (*vide infra*) confirms that **12** possesses a nearly coplanar conformation which should be beneficial to the conjugation. Compound **13**, derived from **11** by replacing the oxadiazolyl core with the better π-accepting pyridazinyl unit,[38] exhibits more a prominent red shift of $\lambda^{(1)}_{abs}$ (433 nm) due to the stronger charge transfer property. Electronic delocalization and charge transfer are favored with the presence of the phenylenevinylene unit in the conjugation bridge, and as expected, compounds **8–10** have the largest $\lambda^{(1)}_{abs}$ among all in this study.

According to the absorption spectra, the emission wavelength ($\lambda^{(1)}_{em}$) also decreases with decreasing donor strength in the homologues, such as **3** > **2** > **1**, **6** > **5** > **4** and **10** > **9** > **8**. In general, compounds with a larger $\lambda^{(1)}_{abs}$ also have a larger $\lambda^{(1)}_{em}$. The fluorescence quantum yields (Φ) of the compounds in CH_2Cl_2 range from 5 to 71%. The decreasing Φ value for the compound possessing a stronger donor in the homologues, **1** > **2** > **3**, **4** > **5** > **6** and **8** > **9** > **10** could be due to the more facile quenching of the emission by the stronger donor *via* electron transfer. Alternatively, a better solute–solvent interaction for the compound with increasing charge transfer may also decrease the quantum yield.[39,40]

TPA cross-sections

Several methods can be used to investigate the two-photon resonance and determine the two-photon absorption cross section (σ). They are (1) nonlinear transmission; (2) up-converted fluorescence emission; (3) transient absorption; and (4) four-wave mixing.[17a] The up-converted fluorescence emission technique, which was adopted in this study, is direct and very convenient. In order to eliminate contributions from the excited-state absorption, a femtosecond (~100 fs) pulsed laser was used for the measurement. The two well characterized TPA chromophores, Coumarin 480 (with a TPA cross section of 168.2 GM)[41] and Rhodamine 6G (with a TPA cross section of 38.67 GM),[42] were used as the references.

The TPA cross-sections of these compounds obtained from the TPEF are listed in Table 1. The TPA cross section per unit mass was also compiled for comparison. TPEF (two-photon emission fluorescence) of compound **13** is displayed in Fig. 1, and representative the two-photon excitation (TPE) spectra (750–840 nm) of the compounds **12** and **13** in CH_2Cl_2 are displayed in Fig. 2. For all molecules, SPEF and TPEF spectra were found to be similar, suggesting that both must relax quickly to the same fluorescence emission state even if the primary excited states obtained by single-photon absorption and two-photon absorption may be different because of the

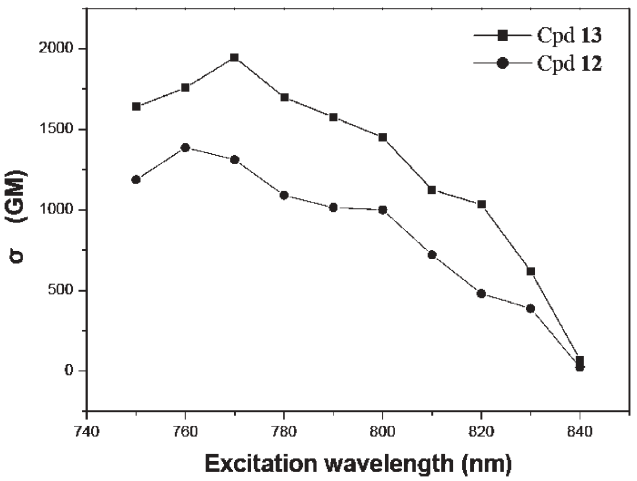

Fig. 2 Two-photon excitation spectra of **12** and **13** in CH_2Cl_2 with $c = 1.0 \times 10^{-4}$ M

different parity selection rules. The TPE peak appears at an energy slightly higher than twice that of the corresponding linear absorption maximum. Significantly large TPA at ~800 nm is very important from the viewpoint of practical applications, because the most frequently used source for the two-photon excitation is the Ti:Sapphire laser, which gives an intense beam at around 800 nm.[17f] A very interesting feature in this study (Fig. 3) is that the TPA cross sections are raised by increasing the donor strength of the arylamines. A significant increment was observed when the naphthyl moiety was

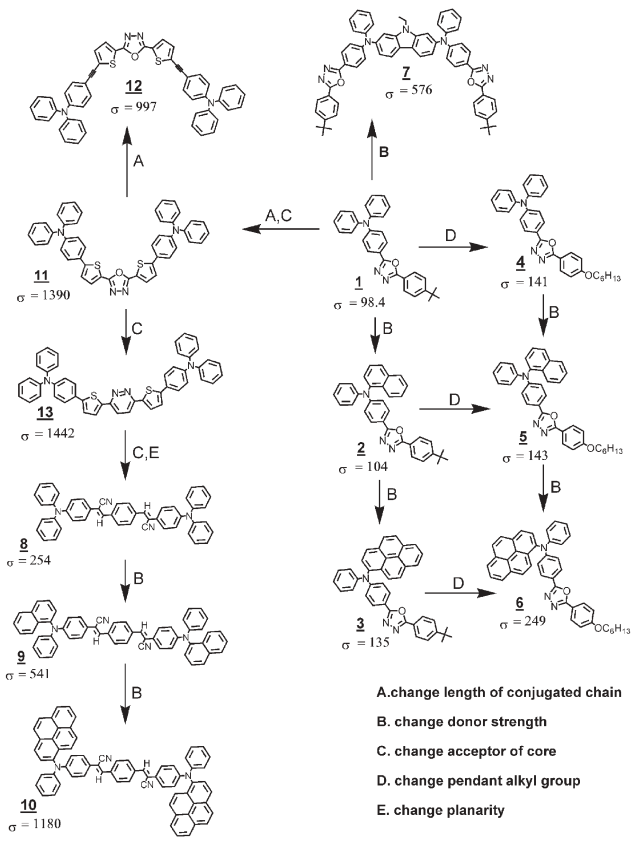

Fig. 3 Flowchart of TPA compounds.

replaced by the pyrenyl moiety, *i.e.*, **2** *vs.* **3**, **5** *vs.* **6** and **9** *vs.* **10**. It is also worth noting that arylamine has a significant effect on the TPA cross sections of the quadrupolar type molecules, **8–10**. Diarylamine has been reported to be a better donor than dialkylamine for TPA chromophores.[17e] Our studies also indicate that further tuning of arylamines is possible for raising the TPA cross section. The TPA cross section per unit mass (σ/MW) also appears to be impressive with such variation of the donor. Both σ and σ/MW values for **9** and **10** are competitive with 9-10-bis(arylethynyl)anthracene-based quadrupolar molecules reported by Jeon and Cho.[30e] It is interesting that **4–6** have significantly higher σ values than **1–3**. In view of the comparable HOMO and LUMO gap between n and n + 3 (n = 1−3),[43] and the weak $n \rightarrow \pi^*$ donating nature of the alkoxy moiety, compounds **4–6**, with a D–π–A–π–D′ backbone, may act as quadrupolar type molecules that normally have a larger TPA effect than dipolar molecules (*vide infra*).

There have been ample examples which demonstrated that the TPA effect could be enhanced from dipolar molecules to quadrupolar analogues.[28–30] For instance, it was found that in homologues with an arylamine donor and oxadiazole acceptor linked by the same conjugated spacer, the quadrupolar compound had a TPA cross section more than double that of the dipolar compound.[28a] Similarly, the octupolar compounds had a TPA cross section more than triple that of the dipolar analogue. Such an effect can be further enhanced by extending the molecules to dendritic structures[30a] or polymers.[30c] We found that the TPA cross section of **7** is almost six times that of **1**. The σ/MW value of **7** is also triple that of **1**. A comparison of **11** with **1**, **4**, and **7** suggests that the TPA effects can be further engineered *via* the modification of the conjugated spacer. The σ value of **11** is nearly double that of **7**. The σ and σ/MW values are impressively raised by 50% when the more electron-deficient pyridazin-3,6-diyl moiety was introduced as the acceptor in replacement of the oxadiazolyl unit (**13** *vs.* **11**).[38] Compound **13** shows the largest TPA cross-section (1442 GM) and σ/MW (1.97) in this study. At this stage, it is not certain why compound **13** has a higher TPA effect than **8–10** despite its shorter $\lambda^{(1)}_{abs}$. Such an outcome might be attributable to the TPEF excitation wavelength (800 nm) being not long enough **8–10** to reach an optimum two-photon excitation. Compound **12** has a smaller TPA cross section than **11**, though the former has a larger $\lambda^{(1)}_{abs}$ due to the presence of an extra ethynyl entity between the central oxadiazole and each of peripheral triphenyl amines. It is likely that the fluorescent state of **13** is better stabilized. The energy mismatch between the ethynyl carbon and aromatic carbon may hinder the electronic communication between the donor and the acceptor and hence reduce the effective conjugation length (ECL) of π-systems.[44]

Structural features of 12

The ORTEP drawing of **12**, $C_{50}H_{32}N_4OS_2{\cdot}2CH_2Cl_2$, is shown in Fig. 4 ($CH_2Cl_2$ molecules have been omitted for clarity). There are no hydrogen bonds between the CH_2Cl_2 solvent and **12** except for a very weak van der Waals intermolecular interaction. For the crystallographic data see †. As shown in Fig. 4, the three phenyl rings of the amino group are arranged in a propeller-like, non-coplanar fashion.[17e,45] Thus, the lone electron pairs in pyramidalization of the NC_3 core may be highly delocalized, mainly toward the acceptor and increase the conjugated strength. The molecular structure of **12** has also been clearly characterized by inspecting the planarity of the several dihedral angles in the molecule. The dihedral angle between the central oxadiazolyl plane (P1) and its neighboring thiophenyl plane (P2) is 6.8(2)°, the dihedral angle between P2 and the phenyl plane (P3) is 9.3(1)°, and that between P1 and P3 is 14.7(2)°. The coplanarity of the molecule should be beneficial to π-delocalization of the system. Fig. 5 (H atoms and CH_2Cl_2 molecules have been omitted for clarity) shows the view along the c axis of the packing diagram of compound **12** in the crystal. By viewing a certain molecular layer (001), we observe that molecules of **12** form a herring-bone like structure and form sheets along the c axis, and that all the main molecular planes are parallel to each other with neighboring molecules arranged in a staggered non-head-to-head manner, the results of which can be attributed to the steric repulsion between the two terminal amino groups.

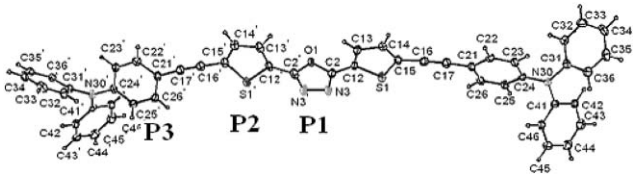

Fig. 4 ORTEP diagram of **12**.

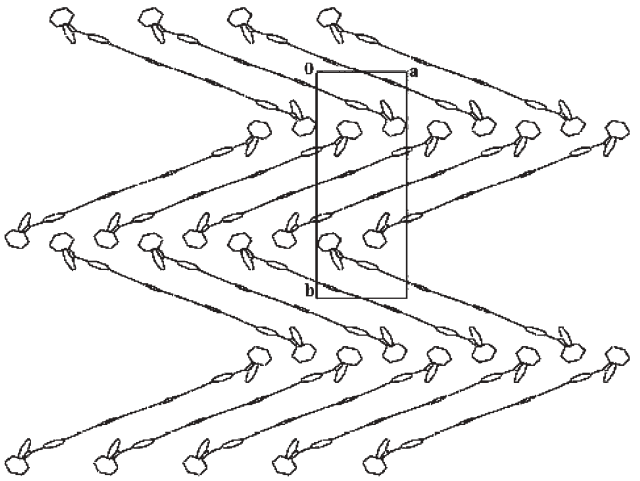

Fig. 5 Packing diagram for **12** viewed along the c axis without solvent molecules.

Conclusions

In summary, we have synthesized series of dipolar and quadrupolar type TPA compounds incorporating various arylamines as electron donors, and [1,3,4]oxadiazolyl, cyanovinyl, or pyridazin-3,6-diyl moieties as the electron acceptors. These compounds were found to have large TPA cross sections determined by the up-converted fluorescence emission method using a femtosecond pulsed laser at 800 nm. Significant

increment of the TPA cross sections can be achieved by incorporation of a pyrenyl unit in the arylamine moiety. By an appropriate combination of the donor and the acceptor, the TPA cross sections can go beyond 10^3 GM. One quadrupolar molecule (compound **13**) possessing an arylamine donor and pyridazine acceptor has the largest TPA cross section per unit mass ever reported. By fixing the pyridazinyl core and testing a series of different donors or structures, we aim to explore new chromophores with stronger TPA and TPEF properties. Work focusing on this issue is currently in progress.

Experimental

General procedures and spectroscopic measurements

Unless otherwise specified, all the reactions were carried out under a nitrogen atmosphere using standard Schlenk techniques. Solvents were dried by standard procedures. All column chromatography was performed with silica gel (230–400 mesh, Macherey-Nagel GmbH & Co.) as the stationary phase. The ^{1}H NMR spectra were recorded on a Bruker AMX400 spectrometer. Electronic absorption spectra were measured in various solvents using a Cary 50 Probe UV–visible spectrophotometer. Emission quantum yields were measured with reference to coumarin 1 or coumarin 6 in CH_3CN.[46] Mass spectra (FAB) were recorded on a JMS-700 double focusing mass spectrometer (JEOL, Tokyo, Japan). Elementary analyses were performed on a Perkin–Elmer 2400 CHN analyzer. 2-(4-bromophenyl)-5-(4-*tert*-butylphenyl)-[1,3,4]oxadiazole,[47] 2-(4-bromophenyl)-5-(4-hexyloxyphenyl)-[1,3,4]oxadiazole,[48] 2,5-bis-(5-bromothiophen-2-yl)-[1,3,4]oxadiazole,[49] 2-(4-bromophenyl)-3-{4-[2-(4-bromophenyl)-2-cyanovinyl]phenyl}acrylonitrile,[50] 3,6-dithiophen-2-yl-pyridazine,[51] 2,7-dibromo-9-ethyl-9*H*-carbazole,[52] and (4-ethynylphenyl)diphenylamine,[53] were prepared by published procedures with slight modifications.

Synthesis of compounds 1–13

Compounds **1–6** and **8–10** were synthesized by a procedure similar to that described in the following. A two-necked round-bottomed flask was charged with $Pd(OAc)_2$ (1 mmol% per halogen atom), *t*-BuONa (1.2 equiv. per halogen atom), the halides (5 mmol), and amines (2 equiv. per halogen atom). Dry toluene was added, and the reaction was stirred under nitrogen for 10 min. Tri-*tert*-butylphosphine (2 mmol%) in dry toluene was added through a syringe (the stock solution contained 1.0 mmol of the phosphine in 1 mL of dry toluene). The reaction mixture was heated at 90 °C for 20 h. After cooling, the mixture was diluted with ether and the organic phase was washed with water and brine. After being dried over $MgSO_4$ and filtered, the volatiles were removed in vacuum and the residue was purified by column chromatography using CH_2Cl_2/*n*-hexane as eluent. The compound was further purified by recrystallization from CH_2Cl_2 and MeOH.

{4-[5-(4-*tert*-Butylphenyl)-[1,3,4]oxadiazol-2-yl]phenyl}diphenylamine (1). Compound **1** was obtained as a pale-white solid in 76% yield. FAB MS: *m*/*e* 446.2 $(M + H)^+$; ^{1}H NMR ($CDCl_3$): 1.35 (s, 9 H, $C(CH_3)_3$), 7.08–7.17 (m, 8 H), 7.30 (t, J = 7.7 Hz, 4 H, C_6H_5), 7.51 (d, J = 8.3 Hz, 2 H, C_6H_4), 7.92 (d, J = 8.6 Hz, 2 H, C_6H_5); 8.01 (d, J = 8.6 Hz, 2 H, C_6H_5); Anal. calc. for $C_{30}H_{27}N_3O$: C, 80.87; H, 6.11; N, 9.43. Found: C, 80.75; H, 6.36; N, 9.62.

{4-[5-(4-*tert*-Butylphenyl)-[1,3,4]oxadiazol-2-yl]phenyl}-naphthalen-1-ylphenylamine (2). Compound **2** was obtained as a pale-yellow solid in 71% yield. FAB MS: *m*/*e* 496.2 $(M + H)^+$; ^{1}H NMR ($CDCl_3$): 1.38 (s, 9 H, $C(CH_3)_3$), 7.01 (d, J = 8.7 Hz, 2 H), 7.10 (t, J = 6.9 Hz, 1 H), 7.22–7.33 (m, 4 H), 7.42 (t, J = 7.1 Hz, 2 H), 7.49–7.55 (m, 4 H), 7.86 (d, J = 8.2 Hz, 1 H), 7.91–7.95 (m, 4 H), 8.03 (d, J = 8.3 Hz, 2 H); Anal. calc. for $C_{34}H_{29}N_3O$: C, 82.40; H, 5.90; N, 8.48. Found: C, 82.49; H, 5.57; N, 8.38.

{4-[5-(4-*tert*-Butylphenyl)-[1,3,4]oxadiazol-2-yl]-phenyl}-(3,5-dihydropyren-1-yl)phenylamine (3). Compound **3** was obtained as a pale-yellow solid in 69% yield. FAB MS: *m*/*e* 572.2 $(M + H)^+$; ^{1}H NMR ($CDCl_3$): 1.29 (s, 9 H, $C(CH_3)_3$), 7.02–7.09 (m, 3 H), 7.22–7.30 (m, 4 H), 7.9 (d, J = 8.1 Hz, 2 H, C_6H_4), 7.85–8.14 (m, 11 H), 8.19 (d, J = 8.0 Hz, 2 H, C_6H_4); Anal. calc. for $C_{40}H_{33}N_3O$: C, 84.03; H, 5.82; N, 7.35. Found: C, 84.42; H, 5.76; N, 7.55.

{4-[5-(4-Hexyloxyphenyl)-[1,3,4]oxadiazol-2-yl]phenyl}diphenylamine (4). Compound **4** was obtained as a pale-white solid in 67% yield. FAB MS: *m*/*e* 490.2 $(M + H)^+$; ^{1}H NMR ($CDCl_3$): 0.88 (t, J = 7.1 Hz, 3 H, CH_3), 1.28–1.42 (m, 4 H), 1.47 (q, J = 6.7 Hz, 2 H), 1.76 (q, J = 6.7 Hz, 2 H), 4.00 (t, J = 6.7 Hz, 2 H, OCH_2), 6.97 (d, J = 8.9 Hz, 2 H, C_6H_4), 7.07–7.15 (m, 8 H), 7.31 (t, J = 7.8 Hz, 4 H), 7.90 (d, J = 8.8 Hz, 2 H, C_6H_4), 8.00 (d, J = 8.8 Hz, 2 H); Anal. calc. for $C_{32}H_{31}N_3O_2$: C, 78.50; H, 6.38; N, 8.58. Found: C, 78.35; H, 6.27; N, 8.65.

{4-[5-(4-Hexyloxyphenyl)-[1,3,4]oxadiazol-2-yl]phenyl}-naphthalen-1-ylphenylamine (5). Compound **5** was obtained as a yellow solid in 77% yield. FAB MS: *m*/*e* 540.2 $(M + H)^+$; ^{1}H NMR (acetone-d_6): δ 8.01 (d, J = 8.6 Hz, 3 H), 7.96–7.89 (m, 4 H), 7.58 (t, J = 7.8 Hz, 1 H, $C_{10}H_7$), 7.52 (t, J = 7.8 Hz, 1 H, $C_{10}H_7$), 7.45–7.41 (m, 2 H), 7.32 (t, J = 7.8 Hz, 2 H), 7.22 (d, J = 7.7 Hz, 2 H), 7.16–7.07 (m, 3 H), 6.96 (d, J = 8.8 H, 2 H), 4.06 (t, J = 6.7 Hz, 2 H), 1.78 (q, J = 6.7 Hz, 2 H), 1.55 (q, J = 6.7 Hz, 2 H), 1.38–1.27 (m, 4 H), 0.87 (t, J = 7.1 Hz, 3 H); Anal. calc. for $C_{36}H_{33}N_3O_2$: C, 89.25; H, 6.46; N, 6.12. Found: C, 88.93; H, 6.12; N, 6.01.

{4-[5-(4-Hexyloxyphenyl)-[1,3,4]oxadiazol-2-yl]phenyl}phenylpyren-1-ylamine (6). Compound **6** was obtained as a yellow-green solid in63% yield. FAB MS: *m*/*e* 614.1 $(M + H)^+$; ^{1}H NMR (acetone-d_6): δ 8.38 (d, J = 8.1 Hz, 1 H), 8.33 (d, J = 7.6 Hz, 1 H), 8.26 (d, J = 7.0 Hz, 1 H), 8.22–8.17 (m, 3 H), 7.37 (t, J = 7.2 Hz, 2 H), 7.30 (d, J = 7.4 Hz, 2 H), 7.16–7.04 (m, 5 H), 4.09 (t, J = 6.7 Hz, 2 H), 1.78 (q, J = 6.7 Hz, 2 H), 1.52 (q, J = 6.7 Hz, 2 H), 1.37–1.26 (m, 4 H), 0.87 (t, J = 7.1 Hz, 3 H); Anal. calc. for $C_{42}H_{35}N_3O_2$: C, 82.19; H, 5.57; N, 6.85. Found: C, 81.82; H, 5.21; N, 6.39.

***N,N′*-Bis-{4-[5-(4-*tert*-butyl-phenyl)-[1,3,4]oxadiazol-2-yl]-phenyl}-9-ethyl-*N,N′*-diphenyl-9*H*-carbazole-2,7-diamine (7).** 2,7-Dibromo-9-ethyl-9*H*-carbazole (2.0 mmol), phenylamine

(4.4 mmol), $Pd(OAc)_2$ (9.2 mg, 0.04 mmol), $(t\text{-}Bu)_3P$, (0.012 g, 0.04–0.06 mmol), sodium- *tert*-butoxide (0.288 g, 3.0 mmol), and toluene (20 mL) were mixed together and heated at 80 °C for 24 h. After cooling, it was quenched with 5 mL of water. The solvent was removed under vacuum and the residue was extracted with dichloromethane/water. The organic layer was dried over $MgSO_4$ and filtered. Evaporation of the solvent left a brown residue that was chromatographed through silica gel using dichloromethane/hexane mixture as eluant. Compound 9-ethyl-*N,N′*-diphenyl-9*H*-carbazole-2,7-diamine (**7a**) was obtained as white solid in 87% yield. FAB MS: *m/e* 377 (M^+); ^{1}H NMR (acetone-d_6): 7.86 (d, J = 8.2 Hz, 2 H), 7.47 (br, 2 H, N*H*), 7.26–7.18 (m, 10 H), 6.97 (d, J = 8.2 Hz, 2 H), 6.80 (t, J = 7.0 Hz, 2 H), 4.28 (q, J = 7.1 Hz, 2 H, CH_2), 1.35 (t, J = 7.1 Hz, 3 H, CH_3); Anal. calc. for $C_{26}H_{23}N_3$: C, 82.73; H, 6.14; N, 11.13; Found: C, 82.93; H, 5.97; N, 10.84.

Compound **7** were synthesized from **7a** by a procedure similar to that of **1–6**. It was isolated as a yellow solid in 83% yield. FAB MS: *m/e* 930 (M^+); ^{1}H NMR (acetone-d_6): 8.13 (d, J = 8.2 Hz, 2 H), 8.06 (d, J = 8.3 Hz, 4 H), 8.00 (d, J = 8.3 Hz, 4 H), 7.67 (d, J = 8.4 Hz, 4 H), 7.44–7.38 (m, 6 H), 7.28 (d, J = 8.2 Hz, 4 H), 7.18–7.16 (m, 6 H), 7.05 (dd, J = 8.3; 1.8 Hz, 2 H), 4.31 (q, J = 7.1 Hz, 2 H, CH_2), 1.37 (s, 18 H, CH_3), 1.27 (t, J = 7.1 Hz, 3 H, CH_3); Anal. calc. for $C_{62}H_{55}N_7O_2$: C, 80.06; H, 5.96; N, 10.54. Found: C, 79.73; H, 5.69; N, 10.61.

2-{4-[1-Cyano-2-(4-diphenylaminophenyl)-vinyl]-phenyl}-3-(4-diphenylaminophenyl)acrylonitrile (8). Compound **8** was obtained as an orange solid in 75% yield. FAB MS: *m/e* 666 (M^+). ^{1}H NMR ($CDCl_3$): δ 7.92 (s, 4 H, C_6H_4), 7.2 (d, J = 8.6 Hz, 4 H, C_6H_4), 7.39 (s, 2 H, C=C*H*), 7.28 (t, J = 7.6 Hz, 8 H, *m*-C_6H_5), 7.12–7.05 (m, 16 H, *o*-C_6H_5, *p*-C_6H_5 and C_6H_4). Anal. calc. for $C_{48}H_{34}N_4$: C, 86.46; H, 5.14; N, 8.40. Found: C, 86.06; H, 5.19; N, 8.29.

2-(4-{1-Cyano-2-[4-(naphthalen-1-ylphenylamino)phenyl]-vinyl}phenyl)-3-[4-(naphthalen-1-ylphenylamino)phenyl]acrylonitrile (9). Compound **9** was obtained as orange solid in 70% yield. FAB MS: m/e 766 (M^+); ^{1}H NMR ($CDCl_3$): δ 7.89 (m, 8 H), 7.81 (d, J = 8.0 Hz, 2 H), 7.51–7.45 (m, 8 H), 7.40–7.34 (m, 6 H), 7.27–7.23 (m, 4 H), 7.14 (d, J = 7.8 H, 4 H), 7.03 (t, J = 7.2 H, 2 H), 6.97 (d, J = 7.2 H, 4 H); Anal. calc. for $C_{56}H_{38}N_4$: C, 87.70; H, 4.99; N, 7.31. Found: C, 87.32; H, 4.73; N, 7.02.

2-(4-{1-Cyano-2-[4-(phenylpyren-1-ylamino)phenyl]vinyl}phenyl)-3-[4-(phenylpyren-1-ylamino)phenyl]acrylonitrile (10). Compound **10** was obtained as yellow solid in 68% yield. FAB MS: m/e 914 M^+; ^{1}H NMR ($CDCl_3$): δ 8.18 (d, J = 7.8 Hz, 4 H), 8.13–8.07 (m, 8 H), 7.99–7.94 (m, 4 H), 7.88 (s, 4 H), 7.83 (d, J = 8.0 Hz, 2 H), 7.48 (d, J = 8.6 Hz, 4 H), 7.32 (s, 2 H), 7.27–7.24 (m, 4 H), 7.17 (d, J = 7.8 H, 4 H) 7.05–6.99 (m, 6 H); Anal. calc. for $C_{68}H_{42}N_4$: C, 89.25; H, 6.46; N, 6.12. Found: C, 88.93; H, 6.12; N, 6.05.

2,5-Bis-[5-(4-diphenylaminophenylethynyl)thiophen-2-yl]-[1,3,4]oxadiazole (11). To a mixture of 2,5-bis-(5-bromothiophen-2-yl)-[1,3,4]oxadiazole (0.39 g, 1.0 mmol), diphenyl-(3-tributylstannanylphenyl)amine (1.12 g, 2.1 mmol) and $PdCl_2(PPh_3)_2$ (28 mg, 0.04 mmol) was added 8 mL of dry dimethylformamide (DMF). The solution was slowly warmed to 80 °C and stirred for 48 h. After cooling, methanol (5 mL) was added to precipitate the product. The solid was filtered, washed with methanol (2 × 5 mL), and then chromatographed using dichloromethane/hexane as eluent. Compound **11** was obtained as an orange solid in 49% yield. FAB MS: *m/e* 721.1 $(M + H)^+$; ^{1}H NMR (CD_2Cl_2): 6.92–7.14 (m, 16 H), 7.25–7.33 (m, 10 H), 7.52 (d, J = 8.6 Hz, 4 H, C_6H_4), 7.67 (d, J = 4.0 Hz, 2 H, SCC*H*); Anal. calc. for $C_{46}H_{32}N_4OS_2$: C, 76.64; H, 4.47; N, 7.77. Found: C, 77.01; H, 4.30; N, 7.45.

2,5-Bis-[5-(4-diphenylaminophenylethynyl)thiophen-2-yl]-[1,3,4]oxadiazole (12). 2,5-Bis-(5-bromothiophen-2-yl)-[1,3,4]-oxadiazole (0.392 g, 1.0 mmol), (4-ethynylphenyl)diphenylamine (0.592 g, 2.2 mmol), $Pd(PPh_3)_2Cl_2$ (21.1 mg, 3 mmol%), CuI (11.7 mg, 6 mmol%), triphenylphosphine (6.55 mg, 2.5 mmol), diethylamine (10 mL) and THF (20 mL) were charged sequentially in a two-neck flask under nitrogen atmosphere and heated to reflux for 24 h. After cooling, the volatiles were removed under vacuum, and the resulting solid was extracted into diethyl ether. The organic extract was washed with brine solution, dried over anhydrous $MgSO_4$ and filtered. Evaporation of the solvent left a brown residue that was chromatographed through silica gel using dichloromethane/hexane mixture as eluant. Compound **12** was obtained as an orange solid in 60% yield. FAB MS: *m/e* 769.1 $(M + H)^+$; ^{1}H NMR (CD_2Cl_2): 6.98 (d, J = 8.8 Hz, 4 H, C_6H_4), 7.08–7.14 (m, 12 H), 7.28–7.34 (m, 10 H), 7.38 (d, J = 8.8 Hz, 4 H, C_6H_4), 7.69 (d, J = 4.0 Hz, 2 H, SCC*H*); Anal. calc. for $C_{50}H_{32}N_4OS_2$: C, 78.10; H, 4.19; N, 7.29. Found: C, 77.97; H, 4.27; N, 7.39.

3,6-Bis-[5-(4-diphenylaminophenyl)thiophen-2-yl]pyridazine (13). To a mixture of 3,6-bis-(5-tributylstannanylthiophen-2-yl)pyridazine (1.25 g, 1.36 mmol, 90% purity), (4-bromophenyl)-diphenylamine (0.90 g, 2.8 mmol) and $PdCl_2(PPh_3)_2$ (28 mg, 0.04 mmol) was added 8 mL of dry dimethylformamide (DMF). The solution was slowly warmed to 80 °C and stirred for 48 h. After cooling, methanol (5 mL) was added to precipitate the product. The solid was filtered, washed with methanol (2 × 5 mL), and then chromatographed using dichloromethane/hexane as eluent. Compound **13** was obtained as yellow solid in 52% yield. FAB MS: *m/e* 731.1 $(M + H)^+$; ^{1}H NMR (CD_2Cl_2): 7.02–7.14 (m, 16 H), 7.28–7.35 (m, 10 H), 7.57 (d, J = 8.6 Hz, 4 H, C_6H_4), 7.62 (d, J = 3.9 Hz, 2 H, SCC*H*), 7.77 (s, 2 H, NCC*H*); Anal. calc. for $C_{48}H_{34}N_4S_2$: C, 78.87; H, 4.69; N, 7.67. Found: C, 78.70; H, 4.39; N, 7.53.

Measurement of two-photon cross section by the two-photon-induced fluorescence method

The setup for the TPEF excitation spectra and TPEF excitation cross-section measurement is depicted in Fig. 6 and is similar to that used by Xu *et al.*[41,54] In brief, a femtosecond mode-locked Ti:sapphire laser (Spectra Physics) generates ~100 fs pulses at repetition rate of 82 MHz with an average power of 300–400 mW. The laser beam was focused on a sample cell (1 cm) by a lens with the focal length 6 cm. To

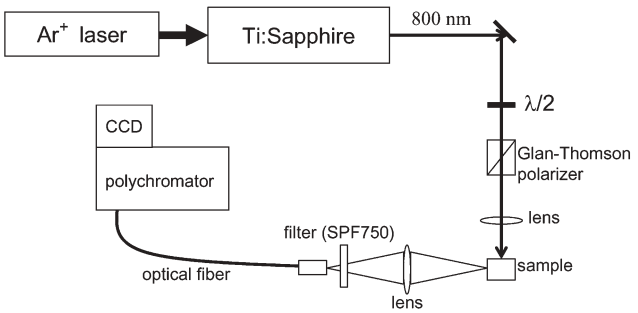

Fig. 6 Experimental setup for TPEF measurement

minimize the effects of re-absorption, the excitation beam was focused as close as possible to the wall of the quartz cell, which faced the slit of the imaging spectrograph. TPEF was detected in a direction perpendicular to the pump beam. The TPEF was focused by a lens with the focal length 8 cm, and was coupled *via* an optical fiber (Acton, ILG-45-20-3) into an optical spectrum analyser. Our optical spectrum analyzer consists of a CCD with detector control (ICCD-576G, Princeton Instruments. Inc.) in conjunction with an monochromator (SpectraPro-275, Acton Reaearch Corporation) was used as a recorder.

The TPA and TPEF cross-sections (σ and σ_e, respectively) are basic parameters to evaluate a material's TPA and TPEF properties. From the TPEF intensity data, σ_e and σ can be evaluated using eqns (1) and (2),[41,54], where r stands for the reference compound, n for the refractive index of the solvent, and F for the integrated fluorescence intensity; the concentration of the molecules in solution is C.

$$\sigma_e = \sigma_{e,r} \frac{F n_r C_r}{F_r n C} \quad (1)$$

$$\sigma \Phi = \sigma_e \quad (2)$$

The TPEF cross-section σ_e is supposed to be linearly dependent on the TPA cross-section (σ) with the TPEF quantum yield Φ' as the coefficient.[41] In most reports, the SPEF quantum yield Φ was adopted instead of Φ', because Φ' is difficult to measure. By referencing the TPEF cross-section of Coumarin 480 to be 146.3 GM (1 GM = 10^{-50} cm^4·s photon^{-1})[42] and Rhodamine 6G to be 37.90 GM (1 GM = 10^{-50} cm^4·s photon^{-1}).[41] The TPA cross-sections of these compounds were obtained (Table 1). The TPEF spectra of all these compounds were taken when they were excited at 800 nm in CH_2Cl_2. The TPEF of Coumarin 480 or Rhodamine 6G was measured as a standard under the same experimental conditions. We obtained the relative TPEF cross-sections σ_e of these compounds by comparing their TPEF to that of Coumarin 480 (compounds **1–7** and **11–13**) or Rhodamine 6G (compounds **8–10**) under exactly the same experimental conditions.

Structural determination of 12

Orange prismatic crystals of **12**[55] with the CH_2Cl_2 solvent located inside the cavities of the chain structure (dimensions 0.22 × 0.16 × 0.12 mm^3), $C_{50}H_{32}N_4OS_2{\cdot}2CH_2Cl_2$, suitable for single-crystal X-ray diffraction were grown by slow evaporation of a solution in CH_2Cl_2 at room temperature. For the crystallographic data see †. The orthorhombic space group $P2_12_12$ was determined from systematic absences of specific reflections; successful refinement of the structure confirmed the space group assignment. All calculations were performed using the SHELX software package by a direct method and refined by a full-matrix least-squares method on F^2.

Acknowledgements

This work is partially supported by the Institute of Chemistry, Academia Sinica, and Department of Chemistry, National Taiwan University, and Department of Chemistry, National Taiwan Normal University, and Kang-Ning Junior College of Medical Care and Management.

References

1 M. Goppert-Mayer, *Ann. Phys. (Leipzig)*, 1931, **9**, 273.
2 W. L. Peticolas, *Annu. Rev. Phys. Chem.*, 1967, **18**, 233.
3 J. D. Bhawalkar, G. S. He and P. N. Prasad, *Rep. Prog. Phys.*, 1996, **59**, 1041.
4 W. Denk, J. H. Stricker and W. W. Webb, *Science*, 1990, **248**, 73.
5 C. W. Spangler, *J. Mater. Chem.*, 1999, **9**, 2013.
6 S. Maruo, O. Nakamura and S. Kawata, *Opt. Lett.*, 1997, **22**, 132.
7 W. Zhou, S. M. Kuebler, K. L. Braum, T. Yu, J. K. Cammack, C. K. Ober, W. Perry and S. R. Marder, *Science*, 2002, **296**, 1106.
8 G. S. He, G. C. Xu, P. N. Prasad, B. A. Reinhardt, J. C. Bhatt and A. G. Dillard, *Opt. Lett.*, 1995, **20**, 435.
9 G. S. He, C. Weder, P. Smith and P. N. Prasad, *IEEE J. Quantum Electron.*, 1998, **34**, 2279.
10 S. W. Hell, P. E. Hanninen, A. Kuusisto, M. Schrader and E. Soini, *Opt. Commun.*, 1995, **117**, 20.
11 J. D. Bhawalkar, N. D. Kumar, J. Swiatkiewicz and P. N. Prasad, *Nonlinear Opt.*, 1998, **19**, 249.
12 M. P. Joshi, H. E. Pudavar, J. Swiatkiewicz, P. N. Prasad and B. A. Reinhardt, *Appl. Phys. Lett.*, 1999, **74**, 170.
13 G. S. He, J. Swiatkiewicz, Y. Jiang, P. N. Prasad, B. A. Reinhardt, L.-S. Tan and R. Kannan, *J. Phys. Chem. A*, 2000, 4805.
14 J. D. Bhawalkar, N. D. Kumar, C. F. Zhao and P. N. Prasad, *J. Clin. Laser, Med. Surg.*, 1997, **15**, 201.
15 B. H. Cumpston, S. P. Ananthavel, S. Barlow, D. L. Dyer, J. E. Ehrlich, L. L. Erskine, A. A. Heikal, S. M. Kuebler, I.-Y. S. Lee, D. McCord-Maughon, J. Qin, H. Röckel, M. Rumi, X.-L. Wu, S. R. Marder and J. W. Perry, *Nature*, 1999, **398**, 51.
16 S. Kawata, H.-B. Sun, T. Tanaka and K. Takata, *Nature*, 2001, **412**, 697.
17 (*a*) B. A. Reinhardt, L. L. Brott, S. J. Clarson, A. G. Dillard, J. C. Bhatt, R. Kannan, L. Yuan, G. S. He and P. N. Prasad, *Chem. Mater.*, 1998, **10**, 1863; (*b*) K. D. Belfield, D. J. Hagan, E. W. Van Stryland, K. J. Schafer and R. A. Negres, *Org. Lett.*, 1999, **1**, 1575; (*c*) K. D. Belfield, K. J. Schafer, W. Mourad and B. A. Reinhardt, *J. Org. Chem.*, 2000, **65**, 4475; (*d*) A. Abbotto, L. Beverina, R. Bozio, A. Facchetti, C. Ferrante, G. A. Pagani, D. Pedron and R. Signorini, *Org. Lett.*, 2002, **4**, 1495; (*e*) D. X. Cao, Q. Fang, D. Wang, Z. Q. Liu, G. Xue, G. B. Xu and W. T. Yu, *Eur. J. Org. Chem.*, 2003, 3628; (*f*) S. K. Lee, W. J. Yang, J. J. Choi, C. H. Kim, S. J. Jeon and B. R. Cho, *Org. Lett.*, 2005, **7**, 323.
18 (*a*) O.-K. Kim, K.-S. Lee, H. Y. Woo, K.-S. Kim, G. S. He, J. Swiatkiewicz and P. N. Prasad, *Chem. Mater.*, 2000, **12**, 284; (*b*) H. M. Kim, M. Y. Jeong, H. C. Ahn, S.-J. Jeon and B. R. Cho, *J. Org. Chem.*, 2004, **69**, 5749; (*c*) P. Shao, B. Huang, L. Chen, Z. Liu, J. Qin, H. Gong, S. Ding and Q. Wang, *J. Mater. Chem.*, 2005, **15**, 4502.
19 M. Rumi, J. E. Ehrlich, A. A. Heikal, J. W. Perry, S. Barlow, Z. Hu, D. McCord-Maughon, T. C. Parker, H. Röckel, S. Thayumanavan, S. R. Marder, D. Beljonne and J.-L. Bredas, *J. Am. Chem. Soc.*, 2000, **122**, 9500.

20 (*a*) L. Ventelon, S. Charier, L. Moreaux, J. Mertz and B. Blachard-Desce, *Angew. Chem., Int. Ed.*, 2001, **40**, 2098; (*b*) O. Mongin, L. Porres, L. Moreaux, J. Mertz and M. Blanchard-Desce, *Org. Lett.*, 2002, **4**, 719.

21 M. Albota, D. Beljonne, J.-L. Bredas, J. E. Ehrlich, J.-Y. Fu, A. A. Heikal, S. E. Hess, T. Kogej, M. D. Levin, S. R. Marder, D. McCord-Maughon, J. W. Perry, H. Röckel, M. Rumi, G. Subramaniam, W. W. Webb, X.-L. Wu and C. Xu, *Science*, 1998, **281**, 1653.

22 R. Kannan, G. S. He, L. X. Yuan, F. Xu, P. N. Prasad, A. G. Dombroskie, B. A. Reinhardt, J. W. Baur, R. A. Vaia and L.-S. Tan, *Chem. Mater.*, 2001, **13**, 1896.

23 L. Ventelon, L. Moreaux, J. Mertz and M. Blanchard-Desce, *Chem. Commun.*, 1999, 2055.

24 B. A. Reinhardt, L. L. Brott, S. J. Clarson, A. G. Dillard, J. C. Bhatt, R. Kannan, L. X. Yuan, G. S. He and P. N. Prasad, *Chem. Mater.*, 1998, **10**, 1863.

25 L. Ventelon, S. Charier, L. Moreaux, J. Mertz and M. Blanchard-Desce, *Angew. Chem., Int. Ed.*, 2001, **40**, 2098.

26 B. R. Cho, K. H. Son, S. H. Lee, Y.-S. Song, Y.-K. Lee, S.-J. Jeon, J. H. Choi, H. Lee and M. Cho, *J. Am. Chem. Soc.*, 2001, **123**, 10039.

27 Z. Q. Liu, Q. Fang, D. Wang, G. Xue, W. T. Yu, Z. S. Shao and M. H. Jiang, *Chem. Commun.*, 2002, 2900.

28 (*a*) P. Macak, Y. Luo, H. Norman and H. Ågren, *J. Chem. Phys.*, 2000, **113**, 7055; (*b*) W. J. Yang, D. Y. Kim, C. H. Kim, M. Y. Jeong, S.-J. Jeon and B. R. Cho, *Org. Lett.*, 2004, **6**, 1389.

29 (*a*) A. Adronov, J. M. Frechet, G. S. He, K.-S. Kim, S.-J. Chung, J. Swiatkiewicz and P. N. Prasad, *Chem. Mater.*, 2000, **12**, 2838; (*b*) W. J. Yang, D. Y. Kim, M. Y. Jeong, H. M. Kim, Y. K. Lee, X. Fang, S. J. Jeon and B. B. Cho, *Chem.–Eur. J.*, 2005, **11**, 4191.

30 (*a*) B. R. Cho, K. H. Son, S. H. Lee, Y.-S. Song, Y.-K. Lee, S.-J. Jeon, J.-H. Choi, H. Lee and M. Cho, *J. Am. Chem. Soc.*, 2001, **123**, 10039; (*b*) W.-H. Lee, H. Lee, J.-A. Kim, J.-H. Choi, M. Cho, S.-J. Jeon and B. R. Cho, *J. Am. Chem. Soc.*, 2001, **123**, 10658; (*c*) B. R. Cho, M. J. Piao, K. H. Son, S. H. Lee, S. J. Yoon, S.-J. Jeon, J.-H. Choi, H. Lee and M. Cho, *Chem.–Eur. J*, 2002, **8**, 3907; (*d*) J. Yoo, S. K. Yang, M.-Y. Jeong, H. C. Ahn, S. J. Jeon and B. R. Cho, *Org. Lett.*, 2003, **5**, 645; (*e*) W. J. Yang, C. H. Kim, M.-Y. Jeong, S. K. Lee, M. J. Piao, S.-J. Jeon, B. R. Cho, S.-J. Jeon and B. R. Cho, *Chem. Mater.*, 2004, **16**, 2783.

31 W.-H. Lee, M. Cho, S.-J. Jeon and B. R. Cho, *J. Phys. Chem.*, 2000, **104**, 11033.

32 K. Sonogashira, Y. Tohda and N. Hagihara, *Tetrahedron Lett.*, 1975, 4467.

33 J. K. Stille, *Angew. Chem., Int. Ed. Engl.*, 1986, **25**, 508.

34 J. F. Hartwig, S. Richard, D. Barahano and F. Paul, *J. Am. Chem. Soc.*, 1996, **118**, 3626.

35 K. R. Justin Thomas, J. T. Lin, Y.-T. Tao and C.-W. Ko, *J. Am. Chem. Soc.*, 2001, **123**, 9404.

36 (*a*) V. P. Rao, Y. M. Cai and A. K.-Y. Jen, *J. Chem. Soc., Chem. Commun.*, 1994, 1689; (*b*) V. P. Rao, A. K.-Y. Jen, K. Y. Wong and K. J. Drost, *J. Chem. Soc., Chem. Commun.*, 1993, 1118; (*c*) Y. Wei, Y. Yang and J.-M. Yeh, *Chem. Mater.*, 1996, **8**, 2659.

37 K. R. Justin Thomas, J. T. Lin, M. Velusamy, Y.-T. Tao and C.-H. Chuen, *Adv. Funct. Mater.*, 2004, **14**, 83.

38 Spartan'04 (semi-empirical, AM1) was used to calculate the energies of pyridazine (the core of **13**) and [1,3,4]oxadiazole (the core of **11**). The pyridazine moiety has a lower LUMO energy (−0.29 eV) than oxadiazole (−0.18 eV).

39 S.-J. Chung, K.-S. Kim, T.-C. Lin, G. S. He, J. Swiatkiewicz and P. N. Prasad, *J. Phys. Chem. B*, 1999, **103**, 10741.

40 P. Macak, Y. Luo, H. Norman and H. Ågren, *J. Chem. Phys.*, 2000, **113**, 7055.

41 M. A. Albota, C. Xu and W. W. Webb, *Appl. Opt.*, 1998, **37**, 7352.

42 W. G. Fisher, E. A. Wachter, F. E. Lytle, M. Armas and C. Seaton, *Appl. Spectrosc.*, 1998, **52**, 536.

43 Spartan'04 (semi-empirical, AM1) was used to calculate the energies of compounds **1**–**6**. Compound **1** has lower LUMO and HOMO energies (−0.90; −8.11 eV) than **4** (−0.87; −8.07 eV), Compound **2** has lower LUMO and HOMO energies (−0.92; −8.06 eV) than **5** (−0.88; −8.04 eV) and **3** has lower LUMO and HOMO energies (−1.02; −8.07 eV) than **6** (−1.01; −8.05 eV).

44 (*a*) A. E. Stiegman, E. Graham, K. J. Perry, L. R. Khundker, L. T. Chen and J. W. Perry, *J. Am. Chem. Soc.*, 1991, **113**, 7658; (*b*) L. T. Cheng, W. Tam, S. H. Stevenson, G. R. Meredith, G. Rikken and S. R. Marder, *J. Chem. Phys.*, 1991, **95**, 10631.

45 X. M. Wang, D. Wang, G. Y. Zhou, W. T. Yu, Y. F. Zhou, Q. Fang and M. H. Jiang, *J. Mater. Chem.*, 2001, **11**, 1600.

46 G. Jones II, W. R. Jackson, C.-y. Choi and W. R. Bergmark, *J. Phys. Chem.*, 1985, **89**, 294.

47 S. Hou and W. K. Chan, *Macromolecules*, 2002, **35**, 850.

48 B. G. Kim, S. Kim and S. Y. Park, *Tetrahedron Lett.*, 2001, **42**, 2697.

49 L. G. Liu, Y. F. Xu, X. H. Qian and Q. C. Huang, *Chin. Chem. Lett.*, 2004, **15**, 7.

50 X. Wu, Y. Liu and D. Zhu, *J. Mater. Chem.*, 2001, **11**, 1327.

51 J. P. Montheard and J. C. Dubois, *J. Heterocycl. Chem.*, 1985, **22**, 719.

52 H. Nishi, H. Kohno and T. Kano, *Bull. Chem. Soc. Jpn.*, 1981, **54**, 1897.

53 M. J. Plater and T. Jackson, *Tetrahedron*, 2003, **59**, 4687.

54 C. Xu and W. W. Webb, *J. Opt. Soc. Am. B*, 1996, **13**, 481.

55 The measurement of compound **12**, $C_{50}H_{32}N_4OS_2{\cdot}2CH_2Cl_2$, formula weight 938.77, was made on a Bruker APEX CCD area-detector diffractometer (Mo Kα radiation, λ = 0.71073 Å). The data were collected at a temperature of 100.0(1) K and the structure was solved by the Direct Method (SIR97) and refined by the full matrix leastsquares method on F^2 with anisotropic temperature factors for non-hydrogen atoms. Hydrogen atoms were located at the calculated positions. An absorption correction was applied using a multiscan procedure. Crystal size: 0.22 × 0.16 × 0.12 mm^3. Orthorhombic, $P2_12_12$, Z = 2. Cell dimensions: a = 9.9509(2), b = 25.1959(5), c = 9.0316(2) Å, α = 90, β = 90, γ = 90°, V = 2264.42(8) Å^3, $2\theta_{max}$ = 50.0°, ρ_{calcd} = 1.377 Mg m^{-3}. A total of 19843 reflections, 3991 were independent (R_{int} = 0.0384), 285 parameters, R_1 = 0.0464 (for reflections with [$I > 2\sigma(I)$]), $w R_2$ = 0.1349 (for all reflections). For the crystallographic data see footnote †.